International Journal of Nanomedicine

Dovepress
open access to scientific and medical research

Open Access Full Text Article

REVIEW

Nanopharmaceuticals (part 2): products in the pipeline

This article was published in the following Dove Press journal:
International Journal of Nanomedicine
11 February 2015
Number of times this article has been viewed

Volkmar Weissig
Diana Guzman-Villanueva

Department of Pharmaceutical Sciences, Midwestern University College of Pharmacy Glendale, Glendale, AZ, USA

Abstract: In part I of this review we assessed nanoscience-related definitions as applied to pharmaceuticals and we discussed all 43 currently approved drug formulations, which are widely publicized as nanopharmaceuticals or nanomedicines. In continuation, here we review the currently ongoing clinical trials within the broad field of nanomedicine. Confining the definition of nanopharmaceuticals to therapeutic formulations, in which the unique physicochemical properties expressed in the nanosize range, when man-made, play the pivotal therapeutic role, we found an apparently low number of trials, which reflects neither the massive investments made in the field of nanomedicine nor the general hype associated with the term "nano." Moreover, after an extensive search for information through clinical trials, we found only two clinical trials with materials that show unique nano-based properties, ie, properties that are displayed neither on the atomic nor on the bulk material level.

Keywords: nanopharmaceuticals, nanomedicine, nanoparticles, nanodrugs, nano-based properties, surface plasmon resonance

Introduction

The National Nanotechnology Initiative (NNI) was launched by the NIH (USA) in 2000 in order to support, coordinate, and advance research and development of nanoscale projects. In part 1 of this review,[1] we assessed the immediate impact of this new program on health science-related research and development. In particular, we discussed the adoption of nanoscience terminology by pharmaceutical scientists, which had resulted in the instantaneous advent of nanopharmaceuticals. In addition, we examined nanoscience-related definitions applied to pharmaceuticals. We had argued that research and development of almost all of the 43 clinically approved drugs, currently publicized as nanopharmaceuticals, had begun long before the launch of the NNI and that in many cases literally only the nanoscience terminology has been adopted by the pharmaceutical science community. Our main conclusion was that the undoubted promise of nanoscience and nanoengineering for the development of novel and highly efficient therapeutics, ie, drugs, is yet to materialize. The promise of nanotechnology for the development of future drugs shall be the focus of this review.

To avoid arbitrary adoptions of nanoscience terminology to physiological macromolecules the size of which happen to be on the nanoscale even after their chemical modification, and at the same time to clarify the scope of our review, we narrowed the definition for nanopharmaceuticals, as discussed in part I. According to Rivera et al[2] nanopharmaceuticals are defined as "pharmaceuticals engineered on the nanoscale, ie, pharmaceuticals in which the nanomaterial plays a pivotal therapeutic role or adds additional functionality to the previous compound". But what exactly are nanomaterials? When reducing this term only to the size range of 1–100 nm, literally all

Correspondence: Volkmar Weissig
Midwestern University College of Pharmacy Glendale, Department of Pharmaceutical Sciences, 19555 N 59th Avenue, Glendale, AZ 85308, USA
Tel +1 623 572 3574
Fax +1 623 572 3565
Email vweiss@midwestern.edu

physiological macromolecules, derivatives, or self-assembled structures thereof would qualify as nanomaterial. Thus, after the inception of the NNI in 2000, the term "nano" was readily adopted for the remaining of the already US Food and Drug Administration (FDA)-approved drugs and drugs under development, as we have discussed previously.[1] Remarkably, however, according to the International Council of Chemical Associations,[3] there is no generally accepted definition of nanomaterials available yet. According to a report given by the National Institute for Occupational Safety and Health in March 2009,[4] the International Organization for Standardization Technical Committee 229 has used the term "nanomaterial" to describe engineered nanoparticles (NPs), which are man-made and designed with unique properties associated with the chemistry of the particles, their size distribution between 1 and 100 nm, shape, and surface characteristics. Stanford University's Department of Environmental Health and Safety[5] lists as examples for engineered nanomaterials fullerenes, carbon nanotubes, metal or metal oxide NPs, and quantum dots.

The unique properties of engineered NPs, which are mainly based on quantum effects and significantly increased surface areas, are displayed neither by the bulk material nor by individual atoms or molecules of that material. "Nanotechnology is not simply working at ever smaller dimensions; rather, working at the nanoscale enables scientists to utilize the unique physical, chemical, mechanical, and optical properties of materials that naturally occur at that scale."[6] We believe that the successful utilization of such unique nanosize-linked properties for the therapy of human diseases is the hallmark of a true nanopharmaceutical.

Our interpretation and definition of nanopharmaceuticals is strengthened by a searchable webpage hosted by the US Nanoscale Science, Engineering, and Technology Subcommittee.[7] This webpage lists hundreds of examples of significant scientific and technological achievements made since the inception of the NNI. According to this source, "these examples provide perspective on how NNI investment in R&D has resulted in significant advances in the field of nanotechnology." However, during a search conducted on May 6, 2014, using "drug, nanodrugs, therapeutics, pharmaceutical, liposome, micelle, albumin, nanomedicine or nanopharmaceutical" as search terms, we found only one example that described the use of carbon nanotube membranes for transdermal drug delivery. None of the 43 drug products currently marketed and widely publicized as nanopharmaceuticals (Table 1 in our previous review[1]) was referenced as an example of "significant advances in the field of nanotechnology." The search under "cancer" resulted in four examples involving implantable microfluidic devices, integrated systems for biomarker detection, microchips for cancer detection, and NP complexes for therapy. The latter, in our opinion a "true nanopharmaceutical," is composed of bioconjugated CdSe/ZnS core–shell quantum dots containing an estradiol moiety. Finally, the search under "polymer" resulted in six examples; however, none of them was remotely related to drug targeting and drug delivery. Certainly, the addition of man-made nonphysiological macromolecules such as polymers and block copolymers[8] to the list of nanoengineered particles has merit. Any nanosized polymer particle has physicochemical properties very different from those of the monomer or the solid bulk material, and the nanosized polymer material also plays a pivotal role in adding new properties to any low-molecular-weight drug. Controlled chemical polymerization reactions, however, go back to the late 1890s before Leo Baekeland's "Bakelite" entered the market in the early 1900s and Herman Staudinger, who coined the term "macromolecule" in the early 1930s.[9] Reclassifying the century-old chemical polymerization reaction as nanoengineering appears as unfitting to us. Therefore, the hugely successful development of polymer therapeutics as nanomedicines, going back to Helmut Ringsdorf in the late 1960s,[10,11] Jindrich Kopecek in the 1970s,[12,13] and Ruth Duncan in the 1980s[14,15] shall not be included here.

In conclusion, the focus of this review will exclusively lie on drug formulations (nanopharmaceuticals), in which unique physicochemical properties of the inorganic nanosized material man-made via nanoengineering play the pivotal therapeutic role. This will include nanotubes, nanoshells, NPs, nanorods, and others, all of which are made from nonphysiological inorganic atomic/molecular or bulk

Table 1 Results of a search of US databases (as indicated in the first row), using the term "nanoparticle" in combination with other terms (as indicated in the first column)

Search terms	Number of hits in ClinicTrials.gov	Number of hits in PubMed.gov
Nanoparticle	169	92,639
Nanoparticle AND iron	19	6,474
Nanoparticle AND gadolinium	2	989
Nanoparticle AND manganese	0	627
Nanoparticle AND gold	3	15,266
Nanoparticle AND silver	8	7,152
Nanoparticle AND silica	5	7,031
Nanoparticle AND titanium	1	3,447
Nanoparticle AND nickel	0	932
Nanoparticle AND hafnium	0	27
Nanoparticle AND carbon	2	10,313

material via nanoengineering methods. Medical nanoproducts and nanodevices (bone substitutes, dental composites, device coatings, in vitro assays and medical dressings, among others), which have been or likely will be approved by the FDA through the 510(k) process, however, shall not be considered.

Nanopharmaceuticals in clinical trials

The results of a targeted search (July 23, 2014) of clinical trials registered at PubMed[16] and at the US National Library of Medicine[17] for nanopharmaceuticals, which could potentially meet our definition, are listed in Table 1. Using "nanoparticle" as the only search term yielded 169 hits; 136 of them, however, involved the combination of nanoparticles with at least one of the search terms "protein, albumin, lipid, nucleic acid, DNA, RNA, and carbohydrate," which we have therefore not considered further.

In the same table we also list the corresponding number of hits found in PubMed. The large numbers in the third column reflect the tremendous efforts currently being undertaken in this field. However, considering the general time it takes to get a drug from the bench into the clinic, it appears that at least another decade has to pass before any of the current intense preclinical developments could reach the market. Table 2 lists details of the clinical trials we identified using the search terms compiled in Table 1, and these will be the basis of our discussion for nanopharmaceuticals "in the pipeline" throughout the remaining part of our review. Information regarding the synthesis and characterization of the nanopharmaceuticals will also be provided.

Iron-based nanoparticles

Five of the 19 listed clinical trials (Table 2) we found using the search term "Nanoparticle AND iron" involved the utilization of protein- or albumin-stabilized NPs and shall therefore be excluded from further discussion. Twelve of the 19 listed clinical trials involved the use of iron oxide NPs for magnetic resonance imaging (MRI). One trial out of the 19 involved the use of iron-bearing NPs for magnetic thermoablation of cancer, and one trial aimed at the development of magnetic biopsy.

Iron-based nanoparticles for magnetic resonance imaging

MRI is used as a powerful diagnostic tool for acquiring 3-D tomographical images of tissues and whole organs at high spatial and temporal resolution. To overcome difficulties in differentiating normal from diseased cells due to small native relaxation time differences, MRI contrast agents are used for the enhancement of imaging sensitivities.[18] Elements of choice for MRI contrast agents are Gd and Fe, two elements possessing a high number of unpaired electrons. Iron oxide as a superparamagnetic agent produces a decrease in the spin–spin relaxation time T_2. Shorter T_2 produces dark T_2 images; therefore, iron oxides are the so-called negative exogenous MRI contrast agents. In contrast, Gd as a paramagnetic agent produces a decrease in spin–lattice relaxation time T_1, causing brighter T_1 images; therefore, Gd is the basis for the so-called positive exogenous MRI contrast agents. The first contrast agent used in the clinic was Gd-DTPA (Magnevist, Schering AG, Berlin, Germany), approved in 1988. Other FDA-approved Gd chelates are Prohance® (BIPSO GmBH, Singen, Germany) and Omniscan® (GE Healthcare, Cork, Ireland), both of which are low-molecular-weight Gd chelates. A significant drawback of Gd chelates is their rapid renal clearance, limiting the time window for MRI. Therefore, over the last decade, efforts have been undertaken to incorporate Gd into or onto NPs such as dendrimers, dextran, polymers, liposomes, and a variety of inorganic NPs (reviewed by Zhu et al[18]). However, as of today, no Gd-based NP has been FDA approved, and there are not even any Gd-NPs undergoing testing in clinical trials. The two trials listed in Table 2 (NCT01973517 and NCT00769093) are using Gd only for comparison with iron oxide NP. Potential advantages of nanomaterial-based MRI contrast agents over low-molecular-weight complexes are, according to Zu et al as follows:[18] First, the possible variety of chemical composition, shapes, and sizes allows for the design of different degrees of biocompatibility and imaging properties. Second, different degrees of biostability can be achieved via specific surface modifications. Third, active targeting of NPs is possible via attaching ligands to the particle surface, and finally, fourth, multimodal imaging can be achieved using a combination of optical and magnetic properties of nanomaterials.

Are iron oxide NPs "true" nanopharmaceuticals that meet the criteria of our definition? They are certainly man-made, albeit only via simple chemical procedures, which do not qualify as nanoengineering methods. The sole property exploited for MRI is the paramagnetism of iron, but this property is also present in the bulk material. Thus, only the size of the material would remain as a basis for classification, yet we have argued that size alone is not sufficient for classifying any agents as nanopharmaceutical. In the case of iron oxide NPs, we believe it is the combination of size and paramagnetism, which is unique and which should perhaps

Table 2 Clinical trials identified using search terms from Table 1

Title (abbreviated)	Condition/purpose	Intervention	Phase (estimated enrollment)	Clinical trial identifier (last verified)/sponsor
Magnetic resonance imaging (MRI)				
Ferumoxytol-Iron Oxide Nanoparticle Magnetic Resonance Dynamic Contrast Enhanced MRI	Primary and nodal tumor imaging; head and neck cancer; metastasis	Ferumoxytol	Phase 0 (20)	NCT01895829 (November 2013) M. D. Anderson Cancer Center
Pre-operative Nodal Staging of Thyroid Cancer using Ultra-Small Superparamagnetic Iron Oxide (USPIO) MRI	Papillary carcinoma of thyroid metastatic to regional lymph node; metastatic medullary thyroid cancer; follicular thyroid cancer lymph node metastasis	Ferumoxytol	(20)	NCT01927887 (August 2013) Massachusetts General Hospital
USPIO Magnetic Resonance Imaging	Cancer of the lymph node	Ferumoxytol	(18)	NCT01815333 (January 2014) M. D. Anderson Cancer Center
Iron Nanoparticle enhanced MRI in the Assessment of Myocardial Infarction	Myocardial inflammation following acute myocardial infarction	Ferumoxytol	Phase 2 (80)	NCT01995799 (November 2013) University of Edinburgh
Ferumoxytol for MRI of Myocardial Infarction	Myocardial infarction	Ferumoxytol	(18)	NCT01323296 (October 2010) University of Edinburgh
Pre-operative Staging of Pancreatic cancer Using SPIO MRI	Pancreatic cancer	Ferumoxytol	Phase 4 (100)	NCT00920023 (March 2013) Massachusetts General Hospital
A Validation Study of MR Lymphangiography Using SPIO, a New Lymphotropic Superparamagnetic Nanoparticle Contrast	Bladder, genitourinary, and prostate cancer; cancer detection in pelvic lymph nodes	Ferumoxtran-10	(10)	NCT00147238 (July 2012) M. D. Anderson Cancer Center
High-Field MRI Iron-Based Contrast-enhanced Characterization of Multiple Sclerosis and Demyelinating Diseases	Multiple sclerosis; ferumoxytol as a marker for active inflammation in multiple sclerosis	Ferumoxytol	(15)	NCT01973517 (April 2014) Stanford University
Ferumoxytol-Enhanced MRI in Adult/Pediatric Sarcomas	Soft tissue sarcomas, imaging of lymph node metastases	Ferumoxytol	(49)	NCT01663090 (November 2012) Dana-Faber Cancer Institute
Assessing Dynamic MRI in Patients with Recurrent High Grade Glioma Receiving Chemotherapy	Brain neoplasm (glioma) imaging	Ferumoxytol	Phase 1 (12)	NCT00769093 (May 2014) OHSU Knight Cancer Institute
Inflammatory Cell Trafficking After Myocardial Infarction	Inflammation during/after myocardial infarction	"Nanoparticles of iron oxide" (not specified)	(Not disclosed)	NCT01127113 (May 2010) University of Edinburgh
Imaging Kidney Transplant Rejection Using Ferumoxytol-Enhanced Magnetic Resonance	Renal transplant rejection, macrophage imaging	Ferumoxytol	(20)	NCT02006108 (July 2014) Stanford University
Magnetic thermoablation				
Magnetic Nanoparticle Thermoablation-Retention and Maintenance in the Prostate	Magnetic thermoablation, prostate cancer	"Magnetic nanoparticles"	Phase 0 (18)	NCT02033447 (January 2014) University College London Hospitals
Magnetic biopsy				
Detection of lymphoblasts by a novel magnetic needle and nanoparticles	Leukemia	CD34-bearing superparamagnetic iron oxide nanoparticles (SPIONs)	Phase 1 (60)	NCT01411904 (April 2011) University of New Mexico
Plasmonic photothermal therapy				
Plasmonic Nanophotothermic Therapy of Atherosclerosis	Stable angina, heart failure, atherosclerosis, multivessel coronary artery disease	Silica–gold iron-bearing nanoparticles	Phase 2 (180)	NCT01270139 (August 2012) Ural State Medical Academy

Plasmonic Photothermal and Stem Cell Therapy of Atherosclerosis	Coronary artery disease, atherosclerosis	Gold nanoparticles with iron oxide–silica shells	Phase 1 (62)	NCT01436123 (October 2012) Ural State Medical Academy
NIR fluorescence imaging				
Targeted Silica Nanoparticle for Image-Guided Intraoperative Sentinel Lymph Node Mapping in Head and Neck Melanoma Patients	Melanoma	Fluorescent cRGDY-PEG-Cy5.5-C dots	Phase 0 (30)	NCT02106598 (October 2014) Memorial Sloan-Kettering Cancer Center
Carbon staining				
Clinical Study on the Harvesting of Lymph Nodes with Carbon Nanoparticles for Advanced Gastric Cancer	Advanced gastric cancer	Carbon nanoparticles	Phase 3 (30)	NCT02123407 (April 2014) Peking University
Radio enhancement				
NBTXR3 Crystalline Nanoparticles and Radiation Therapy in Treating Patients with Soft Tissue Sarcoma of the Extremity	Adult soft tissue sarcoma	Hafnium oxide nanoparticles (NBTXR3) 50 nm spheres, negatively charged surface	Phase 1 (30)	NCT01433068 (January 2014) Nanobiotix

Abbreviations: NIR, near-infrared; PEG, polyethylene glycol.

be accepted as the basis for classifying iron oxide NPs as "true" nanopharmaceuticals. One could even coin the term "nanoparamagnetism," but this might be too much of a stretch of imagination.

Iron oxide NPs are categorized according to their overall hydrodynamic diameter.[19,20] Superparamagnetic iron oxide nanoparticles (SPIONs) have a size bigger than 50 nm. Particles smaller than 50 nm are named ultrasmall superparamagnetic iron oxide nanoparticles (USPIONs), and particles with a hydrodynamic diameter less than 10 nm are called very small superparamagnetic iron oxide particles (VSPIONs).

The unique advantage of iron oxide NPs over low-molecular-weight Gd chelates as MRI contrast agents lies in their avoidance of renal clearance and their swift uptake by the reticuloendothelial system.[21] It has been well established that iron oxide NPs are rapidly taken up by phagocytic cells like Kupffer cells, circulating monocytes/macrophages, mononuclear T cells, reactive astrocytes, microglia, and dendritic cells.[22] Phagocytosis of iron oxide NPs has been shown to increase with particle size. For example, SPIONs with a hydrodynamic diameter of 50–180 nm are more efficiently taken up by phagocytic cells than are USPIONs with sizes of 20–50 nm.[22] This affinity of SPIONs for phagocytic monocytes and macrophages provides the basis for their exploration as labeling agents for activated inflammatory cells such as macrophages and activated microglia. Labeling those cells, in turn, allows the use of MRI for monitoring the involvement of macrophages in inflammatory processes such as multiple sclerosis, stroke, brain tumors, traumatic nerve injury, and vulnerable plaques in carotid artery.[23] It was shown in experimental stroke models that Gd chelates used as MRI contrast agents are not able to differentiate inflamed from noninflamed infarct subareas.[22,24] However, using USPIONs and T_2*-weighted imaging, hypointense areas indicative of USPION-laden inflammatory cells could be visualized.[22]

There are (or have been, respectively) three different iron oxide NP formulations on the market. Feridex® (Advanced Magnetics Inc., Cambridge, MA, USA) was originally FDA approved for liver and spleen MRI, but its manufacturing has been discontinued (for unknown reasons to us) in 2008. Ferumoxytol (or Feraheme™, Amag Pharmaceuticals, Waltham, MA, USA) is FDA approved for iron-replacement therapy, and ferumoxtran-10 (or Combidex®, USA; Sinerem®, Europe) is approved in some European countries for MRI of liver and secondary malignant neoplasms, but never gained approval by the FDA. In the next part of this review, we will briefly describe the synthesis and characterization of these nanopharmaceutical formulations.

Ferumoxytol

Ferumoxytol (Feraheme, Amag Pharmaceuticals) is an FDA-approved aqueous colloidal solution used for the treatment of iron deficiency in adult patients with chronic kidney disease.[25] It consists of USPIONs based on nonstoichiometric magnetite (Fe_3O_4) crystalline cores, coated with polyglucose sorbitol carboxymethylether to minimize the free circulating amount of iron and the possible immunologic responses.[26]

The synthesis of ferumoxytol is carried out by simply mixing divalent and trivalent iron salts and the coating reagent in an aqueous solution, followed by stirring and dropwise addition of a base (commonly, ammonium hydroxide). The mixture is subsequently heated, and the resulting colloidal particles are dialyzed against water for purification.[27,28] Ferumoxytol has been thoroughly characterized by X-ray diffraction analysis, transmission electron microscopy (TEM), dynamic light scattering (DLS), and zeta potential measurements. X-ray diffraction measurements of ferumoxytol have been extensively compared with the iron oxide cores of maghemite and magnetite.[29] Typical ferumoxytol diffractograms show characteristic peaks of X-ray diffraction patterns of magnetite at 56° and 62°, as observed in Figure 1. The presence of sharp peaks at 10°, 20°, and 40° is consistent with the crystalline mannitol included in the ferumoxytol formulation (ferumoxytol for injection contains 44 mg/mL of mannitol). A mean diameter of 6.4 nm for ferumoxytol cores was calculated using the line broadening of the X-ray diffraction patterns, and it was confirmed by TEM[29,30] (see Figure 1).

The hydrodynamic diameter of ferumoxytol, as determined by DLS, was approximately 23 nm, which properly reflects the presence of carbohydrate coating around the iron oxide core. The zeta potential of ferumoxytol NPs measured at acid and basic pH showed negative values.[29] Gel permeation chromatography analysis revealed a molecular weight of approximately 731 kDa. In addition, the ferumoxytol formulation was found to be isotonic, with an osmolality of 291 mOsmol kg^{-1}.[30]

For the assessment of safety (and efficacy for the treatment of anemic chronic kidney disease), 21 patients were treated with ferumoxytol.[31] Patients, divided into two groups, received four intravenous doses of 255 mg (group 1) or two intravenous doses of 510 mg (group 2) of ferumoxytol. Patients of group 1 received ferumoxytol every 2 or 3 days, while group 2 received doses a week apart by an intravenous injection. In order to monitor ferumoxytol safety, the physiological parameters blood pressure, heart rate, respiratory rate, and oral temperature were measured prior, after drug administration, and 8 weeks thereafter. After analyzing the results, it was concluded that no adverse effects were observed, discarding anaphylaxis and hypotension, which have been reported with other iron-bearing formulations. Overall, ferumoxytol was found to be safe at 510 mg dose. Consequently, all the current clinical trials testing ferumoxytol as a MRI contrast agent use doses between 2 and 6 mg/kg, and 510 mg is usually given as the upper limit.

Ferumoxtran-10

Ferumoxtran-10 is a biodegradable USPION composed of monocrystalline magnetite (Fe_3O_4) cores coated with low-molecular-weight dextran T-10.[32,33] These NPs are being investigated as MRI contrast agents to differentiate cancerous from noncancerous lymph nodes. When administered, ferumoxtran-10 accumulates in noncancerous target organs/tissues, enhancing their darkness when imaged by MR. In contrast, cancerous cells, which are unable to uptake the magnetic particles, appear lighter against normal background.[34]

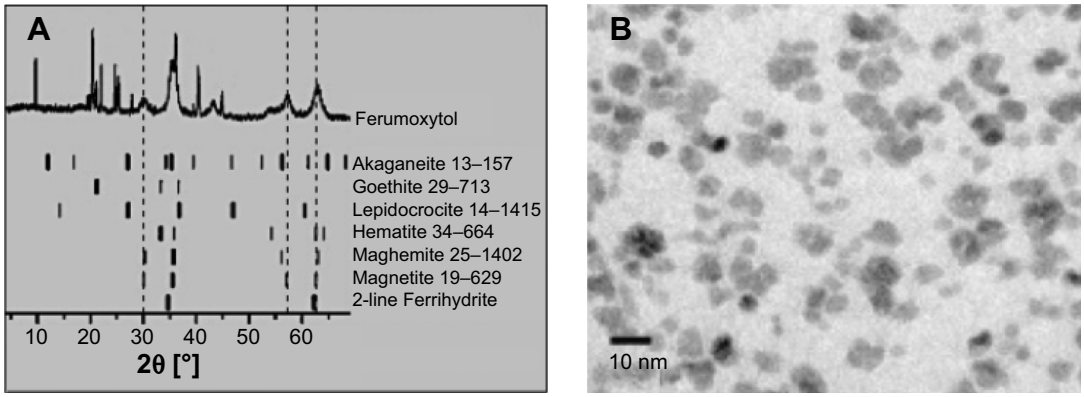

Figure 1 Characterization of ferumoxytol nanoparticles.
Notes: (**A**) X-ray diffraction patterns of ferumoxytol iron oxide nanoparticles, (**B**) TEM of ferumoxytol cores. Reprinted from Elsevier and *European Journal of Pharmaceutics and Biopharmaceutics*, 78(3), Jahn MR, Andreasen HB, Futterer S, et al, A comparative study of the physicochemical properties of iron isomaltoside 1000 (Monofer®), a new intravenous iron preparation and its clinical implications, 480–491, Copyright 2011, with permission from Elsevier.[29]
Abbreviation: TEM, transmission electron microscopy.

Thus, the preferential cellular uptake of ferumoxtran-10 NPs enhances the contrast and the definition of tumor imaging.

The synthesis of ferumoxtran-10 involves the preparation of a solution containing $FeCl_3$ and $FeCl_2$, followed by the addition of a dextran T-10 aqueous solution. Under stirring, a base is added dropwise to neutralize the acidic pH of the solution. During this process, the mixture is heated at 60°C–65°C to obtain homogeneous superparamagnetic iron oxide particles. Finally, the particles are concentrated by ultrafiltration.[35] X-ray diffraction measurements of ferumoxtran-10 revealed diffraction patterns characteristic of crystalline cores of nonstoichiometric magnetite.[36] In addition, small crystallites of ferumoxtran-10 showed a line broadening that was used to calculate their size, which was found to be between 5.8 and 6.2 nm. TEM images of ferumoxtran-10 also confirmed the presence of monocrystalline cores.[36] The size of ferumoxtran-10 cores, as determined by TEM, was found to be 4.3–4.9 nm. On the other hand, the mean hydrodynamic diameter of ferumoxtran-10 particles, determined by DLS, was approximately 20 nm, while the hydrodynamic thickness of the dextran-10 coating was about 8–12 nm.[36] Fourier transform infrared spectroscopy data concluded that dextran-10 partially covers the iron oxide NPs as parts of the particle core have been found to remain uncoated.[37] Figure 2 shows an example of the use of ferumoxtran-10 for lymph node imaging. In this study,[32] 24 healthy volunteers underwent an MR study of the extra cranial neck using ferumoxtran-10 doses of 1.1, 1.7, 2.6, and 3.4 mg Fe/kg. Neck examination was performed 6, 12, 24, and 36 hours after ferumoxtran-10 administration. During the evaluation, it was concluded that the MR images obtained 24 and 36 hours after the administration of 2.6 and 3.4 mg Fe/kg ferumoxtran-10 resulted in the highest specificity to lymph nodes and the best MRI.

Iron-based nanoparticles for magnetic thermoablation

Ferromagnetic materials exposed to a magnetic field with alternating directions dissipate thermal energy as a result of magnetic dipole relaxation following a hysteresis loop. The relaxation of the domain dipole in superparamagnetic species possessing single magnetic domains is known as Néel relaxation.[22] The degree of heating depends on the field strength and the size of the ferromagnetic material. It takes, for example, much lower-strength magnetic fields using VSPIONs (3–7 nm) to achieve the same level of heating as in larger ferromagnetic materials.[22] The general strategy for utilizing this phenomenon for hyperthermic tumor ablation involves either direct inoculation of ferromagnetic NPs into tumor tissues or passive tumor targeting via the Enhanced Permeability and Retention (EPR) effect, followed by applying an alternating magnetic field, which in turn produces an electrical current and subsequent energy dispersion in the form of heat. Currently, there is only one clinical trial registered (NCT02033447, see Table 2) aimed at using this approach to destroy prostate cancer. Detailed information about the magnetic NPs employed by these investigators is unfortunately not available.

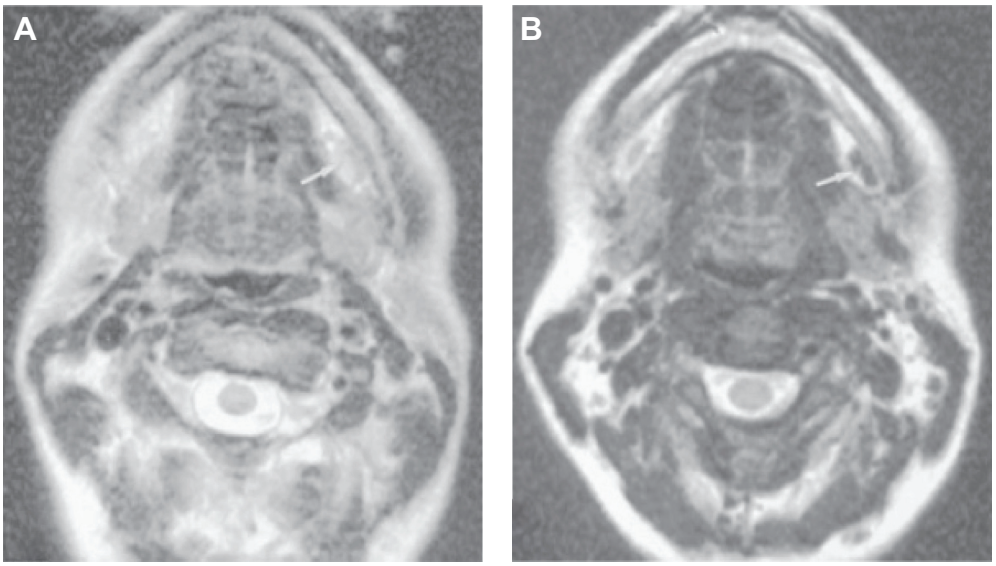

Figure 2 Axial MR imaging of the submandibular node of healthy volunteers after 36 h intravenous administration of Ferumoxtran-10 at a dose of 2.6 mg Fe/kg.
Notes: (**A**) MR imaging without contrast agent and (**B**) enhanced contrast in node using Ferumoxtran-10 nanoparticles. Arrow in panel A indicates node which is difficult to visualize because it is nearly as intense as fat. Arrow in panel B shows excellent contrast between the enhanced left submandibular node and the subcutaneous fat. Republished with permission of *AJNR Am J Neuroradiol*, from Ferumoxtran-10, a superparamagnetic iron oxide as a magnetic resonance enhancement agent for imaging lymph nodes: a phase 2 dose study, Hudgins PA, Anzai Y, Morris MR, Lucas MA, 23(4):649–656, 2002, permission conveyed through Copyright Clearance Center, Inc.[32]

Iron-based nanoparticles for magnetic biopsy

The trial NCT01411904 (Table 2) appears to be the first and only trial employing NPs with a surface modified with cell-specific (antigen-specific) ligands, making it the first and so far only trial (registered at the NIH database) utilizing an active targeting approach.

These CD34-conjugated NPs consist of CD34-conjugated superparamagnetic iron oxide NPs (CD34-SPIONs), used to detect minimal residual disease in leukemia patients through superconductive quantum interference device (SQUID) magnetometry. The SQUID magnometer is a system composed of seven sensors able to detect and measure the magnetic moment of any source placed below the system. CD34-SPION-carrying leukemia cells are collected using a magnetic needle, followed by the magnetization of the NPs using a pulse field, which enables their detection by SQUID as they relax back to equilibrium.[38]

Anti-CD34-conjugated NPs can be prepared by incubating carboxyl groups-bearing commercially available magnetite NPs at an acidic pH and room temperature with EDC and *N*-hydroxysulfosuccinimide, followed by raising the pH to 8 and adding the anti-CD34 antibody.[38,39] TEM studies have shown that the conjugation reaction has no impact on the Ferret diameter of the commercially available NPs. The surface modification with protein (CD34 antibodies), however, increases the particle's hydrodynamic diameter to approximately 70 nm, when measured by DLS.

The magnetic needle used to collect NPs-bearing leukemia cells consists of a bone marrow biopsy-like needle with two magnets attached at the ends of a stainless steel rod, separated from each other by a stainless steel spacer. The CD34-NPs-containing cells are attracted to the magnets in the needle and they are liberated into media to be further analyzed by SQUID relaxometry.[40] In SQUID relaxometry, particles are briefly magnetized by a pulsed magnetic field (approximately 38 Gauss) and detected by magnetization decay over time in a zero field using the SQUID sensor. The SQUID sensor detects only the relaxation times that fall within 50 milliseconds to 2 seconds, as seen in Figure 3. The cell-attached NPs are not free to rotate and get relaxed by the Néel mechanism, thus involving changes in the magnetic moment of the NPs, which results in detectable signal by the SQUID sensor. In contrast, magnetized unbound NPs get relaxed by Brownian rotation of the particles, which is usually too fast to be detected by SQUID.

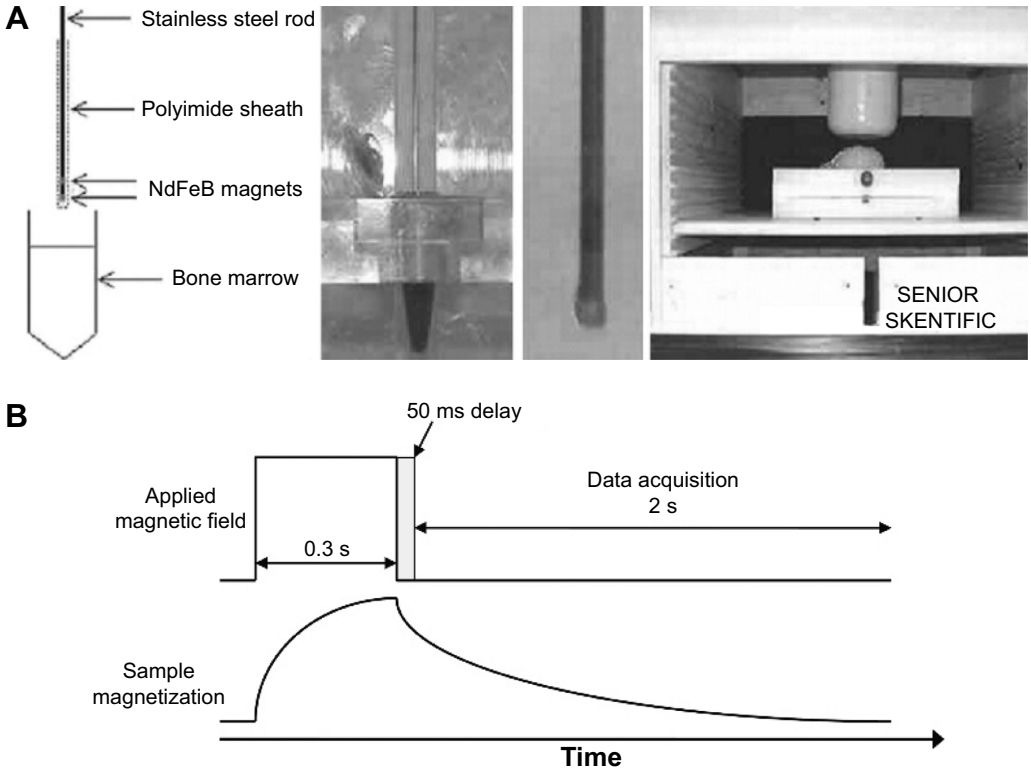

Figure 3 Illustration of SQUID-relaxometry device to detect SPIONs attached to leukemia cells.
Notes: (**A**) Description of the magnetic needle used to acquire samples in leukemia patients, (**B**) Representation of the sample magnetization and data acquisition by SQUID-relaxometry. Reprinted from Elsevier and *Journal of Magnetism and Magnetic Materials*, 321(10), Adolphi NL, Huber DL, Bryant HC, et al, Characterization of magnetite nanoparticles for SQUID-relaxometry, 1459–1464, Copyright 2009, with permission from Elsevier.[39]
Abbreviations: SPIONs, superparamagnetic iron oxide nanoparticles; SQUID, superconductive quantum interference device.

Silica-based nanoparticles

Searching the US database ClinicTrials.gov for registered clinical trials using the search term "Nanoparticle AND silica" yielded 5 trials. One trial involves silica NPs present in clay soil. Another trial involves silica NPs as part of new denture teeth. Two more trials refer to silica as a component of gold NPs used for plasmonic photothermal therapy, already listed in Table 2 (NCT01436123 and NCT01270139) and to be discussed in more detail below under Gold-based nanoparticles. This left only one trial (NCT02106598) that lies within the scope of this review and in which the goal is to explore targeted quantum dots for lymph node imaging in head and neck melanoma patients.[41] The NPs used in this trial are described in the associated trial document as "cRGDY-PEG-Cy5.5-C dots." Such "dots" should not be confused with "quantum dots." Quantum dots are nanocrystals of semiconductors made small enough to exhibit quantum mechanical properties, in particular relating to their excitons, which are the basis for their unique imaging features. The imaging properties of cRGDY-PEG-Cy5.5-C dots, however, are linked to a near-infrared fluorophore, called cyanine 5.5 (Cy5.5), which is covalently attached to the silicon "dot," which, therefore, is "just" a silicon NP and not a silica quantum dot. In addition, these silicon NPs are coated with poly(ethylene glycol) (PEG) chains bearing at the distal end cyclo-[Arg-Gly-Asp-Tyr] (cRGDY) peptides which, in turn, are able to selectively bind to specific integrins, the overexpression of which is associated with neovascularization and proliferation of tumor cells.

Gold-based nanoparticles

One of the three trials found involved the use of organically functionalized gold NPs as sensors for volatile organic compounds, which, together with carbon nanotubes, form the basis for a potential nanomaterial-based breath test. Since gold NPs in this trial are used only in vitro, they fall outside the scope of our review. The remaining two trials utilize gold NPs for plasmonic photothermal therapy, a new approach toward cancer chemotherapy based on the very unique property called "localized surface plasmon resonance" (LSPR), which, in our opinion, is best described by Petryayeva and Krull:

> Localized surface plasmon resonance (LSPR) is an optical phenomenon generated by light when it interacts with conductive nanoparticles (NPs) that are smaller than the incident wavelength. As in surface plasmon resonance, the electric field of incident light can be deposited to collectively excite electrons of a conduction band, with the result being coherent localized plasmon oscillations with a resonant frequency that strongly depends on the composition, size, geometry, dielectric environment and separation distance of NPs.[42]

"Plasmonic" NPs are able to efficiently convert light energy into thermal energy, ie, light into heat, which in turn can be used to destroy cells. When modifying the surface of such NPs with specific cell-recognizing ligands, this technique has the potential to selectively kill cancer (or other target) cells while minimizing undesirable side effects.[43] The unique optical properties of gold NPs which are related to localized plasmonic excitations in metal nanostructures interacting with light[44] are currently under intense investigations as is mirrored by the high number of PubMed hits, as shown in Table 1. A large variety of nanostructures made from gold, including nanoshells, nanorods, nanospheres, and nanocages, have been used as photothermal therapeutic agents for fighting cancers (reviewed by Sikdar et al[45]). In light of the large interest in this new strategy for anticancer therapy, it is surprising (to us) that only two clinical trials are currently listed in the NIH database, both being conducted by the same principal investigator and, moreover, both trials not aiming at destroying cancer cells but exploring LSPR for the treatment of atherosclerosis.[46–48] The type of NPs these investigators are using is not pure gold NPs, but a combination of silica nanocores coated with gold nanoshells (Figure 4).

These gold shell-coated silica particles are synthesized in two steps. First, monodispersed silica NPs are prepared according to the Stöber method, using an excess of tetraethylorthosilicate added to an ethanol and water solution in the presence of ammonia as the catalyst agent.[49] Second, for coating with the gold nanoshell, an aqueous solution of $HAuCl_4$ is rapidly added and mixed with the silica particles in the presence of the reductant and stabilizer agent azacryptand (1,4,7,10,13,16,21,24-octaazabicyclo[8.8.8]hexacosane), as described in Figure 4.[50] The morphology and particle size of the synthesized silica–gold NPs have been analyzed by scanning electron microscopy, revealing a spherical shape with a particle size around 60/15 to 70/40 nm, core/shell, respectively, and the surface plasmon resonance was found to lie around 815–821 nm.[47]

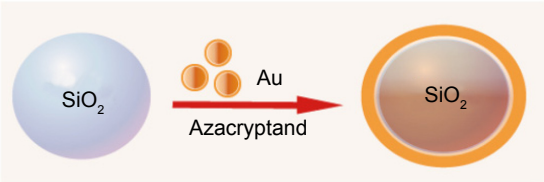

Figure 4 Schematic representation of synthesis of silica–gold nanoparticles.

In order to evaluate the effect of silica–gold NPs in atherosclerotic plaque reduction, miniature swine with advanced plaques, calcium deposits, and intraplaque hemorrhage were used. The animals were treated with silica–gold NPs delivered inside stem progenitor cells, silica–gold iron-bearing NPs using field-assisted delivery, or the control sirolimus-eluting stent, followed by near-infrared laser irradiation (821 nm, 35–44 W/cm^2, 7 minutes) to activate the NPs.[48] Measurements of the plaque vessel, total atheroma, and lumen volume were carried out immediately, and at 3 and 6 months after the procedure. Significant changes in total atheroma volume and percent atheroma volume were observed after laser radiation at 6-month follow-up in animals treated with the silica–gold NPs using the stem cells as carriers. Histological changes and calcium degradation were also observed after the plasmonic photothermal therapy with silica–gold NPs. Overall, around 40%–70% regression of atheroma was obtained.[48]

For further reading on the currently ongoing translational research involving gold NPs, two recently published very comprehensive review articles are recommended.[51,52]

Hafnium-based nanoparticles

Nanoparticles with high electron density allow the deposit of large amounts of energy within living cells when activated by ionizing radiation.[53] In particular, surface-modified negatively charged NPs made of hafnium oxide ("NBTXR3," see Table 2) are currently being explored as selective radio enhancers for the local treatment of solid tumors.[53,54] Upon activation with ionizing radiation, these electron-dense particles generate large quantities of reactive oxygen species inside the tumor, which in turn are ultimately responsible for the cellular damage. The general approach of using NP-based radio enhancers is illustrated in Figure 5.

NBTXR3 NPs are prepared by mixing a solution of tetramethylammonium hydroxide (TMAOH) with hafnium chloride ($HfCl_4$) at a pH in a range between 7 and 13. For crystallization, the white precipitate obtained after the addition of TMAOH is then autoclaved at temperatures between 120°C and 300°C. After cooling, the suspension is washed with water to remove impurities, followed by a peptization process to stabilize the NP suspension. Finally, sodium trimetaphosphate is added and the pH adjusted to 6.7–7.5.[54,55] Transmission electron microscopy of NBTXR3 NPs shows the presence of NPs with a spherical shape as well as the formation of clusters or aggregates.[55] The particle size of hafnium oxide NPs, measured by DLS, revealed a hydrodynamic diameter of 50 nm and a polydispersity index around 0.100, with a negatively charged surface (–50 mV), as estimated by zeta potential measurements. The negative surface charge of NBTXR3 NPs provides them with stability in aqueous solutions with pH ranging from 6 to 8.[53] The cellular uptake of the NBTXR3 NPs has been studied for a variety of cell lines, including epithelial, mesenchymal, and glioblastoma human cancer cells. It was observed that the NPs were taken by the

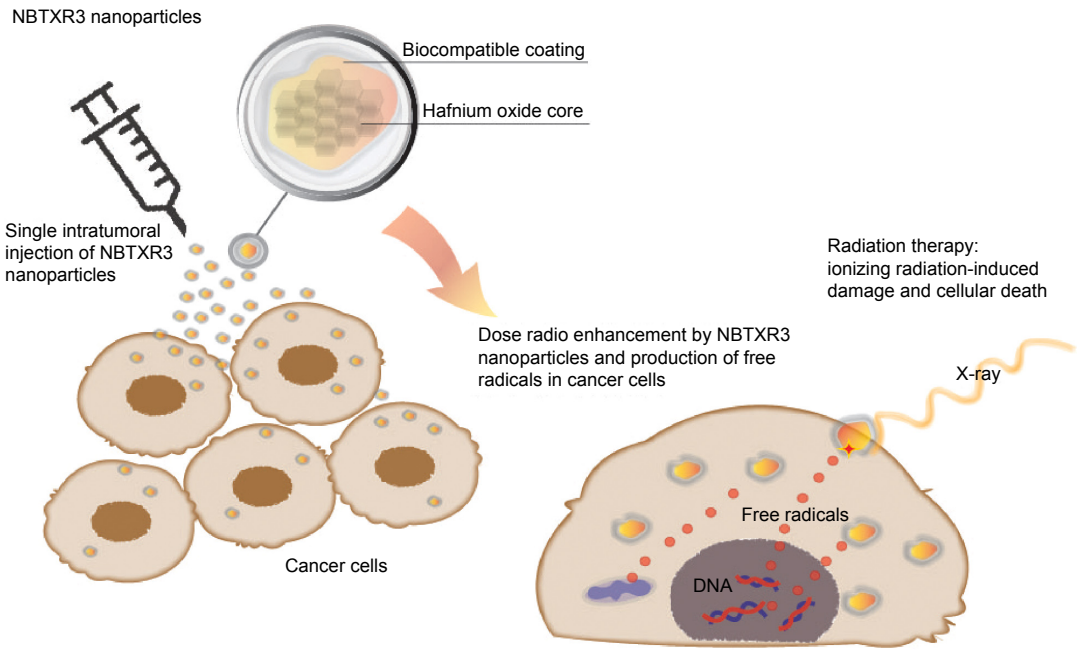

Figure 5 Schematic representation of the radio enhancement mechanism of NBTXR3 nanoparticles in cancer cells after an intratumoral injection.

cells and that, once in cytoplasm, they showed the tendency to form clusters. It was also determined that the NBTXR3 NP uptake was cell line-dependent and that mesenchymal and glioblastoma cell lines showed higher NP uptake.[56]

The antitumor activity of the NBTRX3 NPs was investigated in epithelial xenograft tumor models in SWISS mice.[56] Following a single intratumoral injection of NBTRX3 particles or 5% glucose solution, mice were irradiated with two sessions of 4 Gy or one session of 8 Gy. After the treatment, the weight and the tumor volume were measured twice per week for 25 days and the tumor regrowth delay was determined. As seen in Figure 6, significant antitumor activity was achieved when NBTRX3 NPs were used, compared to irradiation alone. The results were confirmed by Kaplan–Meier curves, which showed that the NBTRX3 NPs markedly increased the cell survival of the animals due to the radio enhancement produced by the particles.

Conclusion and outlook

We have reviewed the currently ongoing clinical trials within the broad field of nanomedicine, confining the definition of nanopharmaceuticals to therapeutic formulations, in which unique physicochemical properties of the nanosized material man-made via nanoengineering play the pivotal therapeutic role. We found that the low number of trials reflects neither the massive investments made in the field of nanomedicines nor the general hype associated with the term "nano." Moreover, when trying to identify those clinical trials utilizing these unique nano-based properties, we found only two trials which involved the use of gold NPs (NCT01270139 and NCT01436123, Table 2). The therapeutic mechanisms of action of these particles are based on the LSPR, an optical property solely displayed by particles at the nanoscale. In contrast, all trials involving the use of iron oxide NPs for MRI, thermoablation, and magnetic biopsy are based on magnetism,

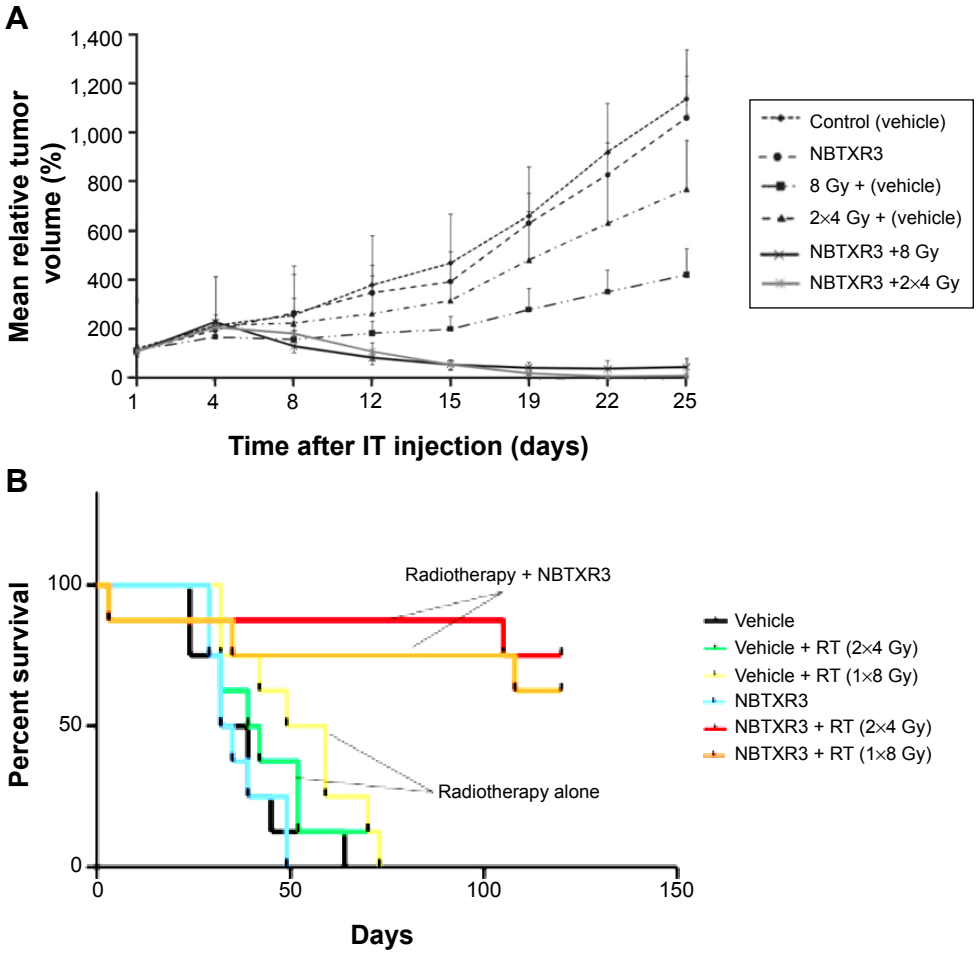

Figure 6 Antitumor activity of NBTXR3 nanoparticles.

Notes: (**A**) Tumor regrowth delay in an HCT 116 epithelial model after NBTXR3 nanoparticle activation. (**B**) Kaplan–Meier curves showing the survival rate of Swiss-mice nude mice after nanoparticle treatment. Copyright © 2012. Reproduced from Maggiorella L, Barouch G, Devaux C, et al. Nanoscale radiotherapy with hafnium oxide nanoparticles. *Future Oncol*. 2012;8(9):1167–1181.[56]

Abbreviations: IT, intratumoral; RT, radiotherapy; HCT, Human Colorectal Tumor cell line.

a property the nanosized and the bulk material have in common. Nevertheless, as can be concluded from Table 1, tremendous efforts are underway worldwide, at the bench and in preclinical research, in order to make the big promise of the nano revolution a reality. We are sure, a similar review to be written about 10 years from now will paint a very different picture and the therapeutic use of true nanopharmaceuticals will have become common clinical practice.

Acknowledgment

The authors gratefully acknowledge the postdoctoral fellowship for Diana Guzman-Villanueva received from the College of Pharmacy at Midwestern University Glendale.

Disclosure

The authors report no conflicts of interest in this work.

References

1. Weissig V, Pettinger TK, Murdock N. Nanopharmaceuticals (part I): products on the market. *Int J Nanomedicine*. 2014;9:4357–4373.
2. Rivera Gil P, Huhn D, del Mercato LL, Sasse D, Parak WJ. Nanopharmacy: inorganic nanoscale devices as vectors and active compounds. *Pharmacol Res*. 2010;62(2):115–125.
3. International Council of Chemical Associations [homepage on the Internet]. Available from: http://www.icca-chem.org/. Accessed September 18, 2014.
4. National Institute for Occupational Safety and Health [homepage on the Internet]. Available from: http://www.cdc.gov/niosh/docs/2009-125. Accessed September 18, 2014.
5. Stanford University Environmental Health [homepage on the Internet]. Available from: http://www.stanford.edu/dept/EHS/prod/. Accessed September 18, 2014.
6. Nano.gov [homepage on the Internet] National Nanotechnology Initiative. Available from: http://www.nano.gov/nanotech-101/special. Accessed September 18, 2014.
7. Nano.gov [homepage on the Internet] Available from: http://www.nano.gov/nanotechnology-initiative/nano-achievements/nanotechnology-initiatives/nano-achievements. Accessed May 6, 2014.
8. Duncan R, Ringsdorf H, Satchi-Fainaro R. Polymer therapeutics-polymers as drugs, drug and protein conjugates and gene delivery systems: past, present and future opportunities. *J Drug Target.* 2006;14(6):337–341.
9. Staudinger H. Viscosity investigations for the examination of the constitution of natuatrl products of high molecualr weight and of rubber and cellulose. *Trans Faraday Soc*. 1933;29:18–32.
10. Batz HG, Franzmann G, Ringsdorf H. Model reactions for synthesis of pharmacologically active polymers by way of monomeric and polymeric reactive esters. *Angew Chem Int Ed Engl*. 1972;11(12):1103–1104.
11. Ringsdorf H. Macromolecular compounds as potential protective agents against ionizing rays. *Strahlentherapie*. 1967;132:627–635.
12. Kopecek J. Soluble biomedical polymers. *Polimery w Medycynie*. 1977;7:191–221.
13. Kopecek J. Controlled biodegradability of polymers-a key to drug delivery systems. *Biomaterials*. 1984;5:19–25.
14. Duncan R. Biological effects of soluble synthetic polymers as drug carriers. *Crit Rev Ther Drug Carrier Syst*. 1985;1(4):281–310.
15. Kopecek J, Rejmanova P, Duncan R, Lloyd JB. Controlled release of drug model from N-(2-hydroxypropyl)-methacrylamide copolymers. *Ann N Y Acad Sci.* 1985;446:93–104.
16. PubMed.gov [homepage on the Internet] Clinical Trails. Available from http://clinicaltrials.gov/. Accessed May 5, 2014.
17. US National Library of Medicine National Institutes of Health [homepage on the Internet]. Available from http://www.ncbi.nlm.nih.gov/pubmed/. Accessed September 8, 2014.
18. Zhu D, Liu F, Ma L, Liu D, Wang Z. Nanoparticle-based systems for t1-weighted magnetic resonance imaging contrast agents. *Int J Mol Sci.* 2013;14(5):10591–10607.
19. Mandarano G, Lodhia J, Eu P, Ferris NJ, Davidson R, Cowell SF. Development and use of iron oxide nanoparticles (Part 2): the application of iron oxide contrast agents in MRI. *Biomed Imaging Interv J*. 2010;6:1–14.
20. Corot C, Robert P, Idee JM, Port M. Recent advances in iron oxide nanocrystal technology for medical imaging. *Adv Drug Deliv Rev*. 2006;58(14):1471–1504.
21. Bourrinet P, Bengele HH, Bonnemain B, et al. Preclinical safety and pharmacokinetic profile of ferumoxtran-10, an ultrasmall superparamagnetic iron oxide magnetic resonance contrast agent. *Invest Radiol*. 2006;41(3):313–324.
22. Weinstein JS, Varallyay CG, Dosa E, et al. Superparamagnetic iron oxide nanoparticles: diagnostic magnetic resonance imaging and potential therapeutic applications in neurooncology and central nervous system inflammatory pathologies, a review. *J Cereb Blood Flow Metab*. 2010;30(1):15–35.
23. Wang YX. Superparamagnetic iron oxide based MRI contrast agents: current status of clinical application. *Quant Imaging Med Surg.* 2011;1(1):35–40.
24. Schroeter M, Franke C, Stoll G, Hoehn M. Dynamic changes of magnetic resonance imaging abnormalities in relation to inflammation and glial responses after photothrombotic cerebral infarction in the rat brain. *Acta Neuropathol*. 2001;101(2):114–22.
25. Bullivant JP, Zhao S, Willenberg BJ, Kozissnik B, Batich CD, Dobson J. Materials characterization of Feraheme/ferumoxytol and preliminary evaluation of its potential for magnetic fluid hyperthermia. *Int J Mol Sci.* 2013;14(9):17501–17510.
26. Provenzano R, Schiller B, Rao M, Coyne D, Brenner L, Pereira BJ. Ferumoxytol as an intravenous iron replacement therapy in hemodialysis patients. *Clin J Am Soc Nephrol.* 2009;4(2):386–393.
27. Weissleder R, Elizondo G, Wittenberg J, Rabito CA, Bengele HH, Josephson L. Ultrasmall superparamagnetic iron oxide: characterization of a new class of contrast agents for MR imaging. *Radiology.* 1990;175(2):489–493.
28. Paul KG, Frigo TB, Groman JY, Groman EV. Synthesis of ultrasmall superparamagnetic iron oxides using reduced polysaccharides. *Bioconjug Chem.* 2004;15(2):394–401.
29. Jahn MR, Andreasen HB, Futterer S, et al. A comparative study of the physicochemical properties of iron isomaltoside 1000 (Monofer), a new intravenous iron preparation and its clinical implications. *Eur J Pharm Biopharm.* 2011;78(3):480–491.
30. Balakrishnan VS, Rao M, Kausz AT, et al. Physicochemical properties of ferumoxytol, a new intravenous iron preparation. *Eur J Clin Invest.* 2009;39(6):489–496.
31. Spinowitz BS, Schwenk MH, Jacobs PM, et al. The safety and efficacy of ferumoxytol therapy in anemic chronic kidney disease patients. *Kidney Int.* 2005;68(4):1801–1807.
32. Hudgins PA, Anzai Y, Morris MR, Lucas MA. Ferumoxtran-10, a superparamagnetic iron oxide as a magnetic resonance enhancement agent for imaging lymph nodes: a phase 2 dose study. *AJNR Am J Neuroradiol*. 2002;23(4):649–656.
33. Muller K, Skepper JN, Posfai M, et al. Effect of ultrasmall superparamagnetic iron oxide nanoparticles (Ferumoxtran-10) on human monocyte-macrophages in vitro. *Biomaterials*. 2007;28:1629–1642.
34. Groman EV, Josephson L, Lewis JM, inventors; Advanced Magnetics, Incorporated, assignee. Magnetic resonance imaging. United States patent US4827945 A. May 9, 1989.

35. Molday RS, Molday LL. Separation of cells labeled with immunospecific iron dextran microspheres using high gradient magnetic chromatography. *FEBS Lett*. 1984;170(2):232–238.
36. Jung CW, Jacobs P. Physical and chemical properties of superparamagnetic iron oxide MR contrast agents: ferumoxides, ferumoxtran, ferumoxsil. *Magn Reson Imaging*. 1995;13(5):661–674.
37. Jung CW. Surface properties of superparamagnetic iron oxide MR contrast agents: ferumoxides, ferumoxtran, ferumoxsil. *Magn Reson Imaging*. 1995;13(5):675–691.
38. Jaetao JE, Butler KS, Adolphi NL, et al. Enhanced leukemia cell detection using a novel magnetic needle and nanoparticles. *Cancer Res*. 2009;69(21):8310–8316.
39. Adolphi NL, Huber DL, Bryant HC, et al. Characterization of single-core magnetite nanoparticles for magnetic imaging by SQUID relaxometry. *Phys Med Biol*. 2010;55(19):5985–6003.
40. Adolphi NL, Huber DL, Jaetao JE, et al. Characterization of magnetite nanoparticles for SQUID-relaxometry and magnetic needle biopsy. *J Magn Magn Mater*. 2009;321:1459–1464.
41. Bradbury MS, Phillips E, Montero PH, et al. Clinically-translated silica nanoparticles as dual-modality cancer-targeted probes for image-guided surgery and interventions. *Integr Biol (Camb)*. 2013;5(1):74–86.
42. Petryayeva E, Krull UJ. Localized surface plasmon resonance: nanostructures, bioassays and biosensing – a review. *Anal Chim Acta*. 2011;706:8–24.
43. Cobley CM, Au L, Chen J, Xia Y. Targeting gold nanocages to cancer cells for photothermal destruction and drug delivery. *Expert Opin Drug Deliv*. 2010;7(5):577–587.
44. Khlebtsov N, Bogatyrev V, Dykman L, et al. Analytical and theranostic applications of gold nanoparticles and multifunctional nanocomposites. *Theranostics*. 2013;3:167–180.
45. Sikdar D, Rukhlenko ID, Cheng W, Premaratne M. Effect of number density on optimal design of gold nanoshells for plasmonic photothermal therapy. *Biomed Opt Express*. 2013;4(1):15–31.
46. Kharlamov AN. Plasmonic photothermal therapy for atheroregression below Glagov threshold. *Future Cardiol*. 2013;9(3):405–425.
47. Kharlamov AN, Tyurnina AE, Veselova VS, Novoselova OS, Filatova AS. Plasmonics for treatment of atherosclerosis: Results of NANOM-FIM trial. *J Nanomed Nanotechnol*. 2013;4:160.
48. Kharlamov AN, Gabinsky JL. Plasmonic photothermic and stem cell therapy of atherosclerotic plaque as a novel nanotool for angioplasty and artery remodeling. *Rejuvenation Res*. 2012;15:222–230.
49. Stoeber W, Fink A, Bohn E. Controlled growth of monodisperse silica spheres in the micron size range. *J Colloid Interface Sci*. 1968;26:62–69.
50. Lee KY, Lee YW, Kwon K, Heo J, Kim J, Han SW. One-step fabrication of gold nanoparticles-silica composites with enhanced catalytic activity. *Chem Phys Lett*. 2008;453:77–81.
51. Bao C, Conde J, Polo E, et al. A promising road with challenges: where are gold nanoparticles in translational research? *Nanomedicine (London)*. 2014;9(15):2353–2370.
52. Conde J, Dias JT, Moros M, Baptista PV, de la Fuente JM. Revisiting 30 years of biofunctionalization and surface chemistry of inorganic nanoparticles for nanomedicine. *Front Chem*. 2014;2:1–27.
53. Marill J, Anesary NM, Zhang P, et al. Hafnium oxide nanoparticles: toward an in vitro predictive biological effect? *Radiat Oncol*. 2014;9:150.
54. Pottier A, Borghi E, Levy L. New use of metals as nanosized radioenhancers. *Anticancer Res*. 2014;34:443–453.
55. Levy L, Pottier A, Rouet A, Marill J, Devaux C, Germain M, inventors; Nanobiotix, assignee. Inorganic nanoparticles of high density to destroy cells in vivo. United States patent US8845507B2. June 4, 2009.
56. Maggiorella L, Barouch G, Devaux C, et al. Nanoscale radiotherapy with hafnium oxide nanoparticles. *Future Oncol*. 2012;8(9):1167–1181.